JAERI-M
9787

INTERNAL DISRUPTION IN HIGH β_P TOKAMAK

November 1981

Masafumi AZUMI, Shinji TOKUDA, Gen-ichi KURITA,
Toshihide TSUNEMATSU, Tomonori TAKIZUKA,
Takashi TUDA, Kimitaka ITOH, Yukio TANAKA*
and Tatsuoki TAKEDA

日本原子力研究所
Japan Atomic Energy Research Institute

JAERI-M 9787

Internal Disruption in High β_p Tokamak

Masafumi AZUMI, Shinji TOKUDA, Gen-ichi KURITA,
Toshihide TSUNEMATSU, Tomonori TAKIZUKA, Takashi TUDA,
Kimitaka ITOH, Yukio TANAKA* and Tatsuoki TAKEDA

Division of Thermonuclear Fusion Research,
Tokai Research Establishment, JAERI

(Received October 20, 1981)

The m = 1 MHD activity is investigated from the veiwpoint of the suppression of the internal disruption and the appearance of large amplitude oscillations observed in the recent high β tokamak experiment. The stabilization of the m = 1 internal kink mode by the toroidal effect is confirmed by using the revised version of ERATO. The nonlinear evolution of the resistive internal kink mode is investigated and the reasonable saturation of the m = 1 magnetic island is obtained by using the new reduced set of equations. The effect of the toroidal coupling between the m = 1 and m = 2 tearing modes is also studied. The m = 2 mode is strongly affected, but the saturation of the m = 1 magnetic island is not realized.

Keywords: Internal Disruption, Tokamak, MHD Stability, High Beta Plasma, Resistive Internal Kink Mode, Toroidal Coupling, ERATO Code, New Reduced Set of Equations

---

* On leave from Fujitsu Ltd.

高β_Pトカマクにおけるインターナル・ディスラプション

日本原子力研究所東海研究所核融合研究部

安積　正史・徳田　伸二・栗田　源一

常松　俊秀・滝塚　知典・津田　　孝

伊藤　公孝・田中　幸夫*・竹田　辰興

（1981年10月20日受理）

最近高ベータ・トカマク実験で観測されたインターナル・ディスラプションの抑制と高振幅振動の発生を説明するために，m＝1モードのMHD挙動が調べられた。トロイダル効果によってm＝1インターナル・キンク・モードが安定化されることが，改訂版ERATOコードによる計算で確認された。抵抗性インターナル・モードの非線形時間発展が調べられ，妥当な大きさのm＝1磁気島の飽和が観測されることが，新簡約方程式系を用いて示された。m＝1およびm＝2ティアリング・モード間のトロイダル・カップリングの効果もまた調べられた。これにより，m＝2モードは強い影響を受けることが示されたが，m＝1磁気島は飽和しなかった。

＊　外来研究員；富士通（株）

Contents

目　　次

1. Introduction

The internal disruption was first observed in the ST tokamak as sawtooth oscillations on soft X-ray signals[1] and, thereafter, it has been commonly observed in tokamaks with the q-value less than unity at the magnetic axis. Since the plasma deformation is restricted within a volume of a critical radius ($\sim \sqrt{2} r_s$, r_s ; the radius of the q = 1 surface), the effect on the plasma confinement is not serious in high-q discharges. In very low-q discharges, however, the energy confinement time is considerably reduced by the sawtooth oscillations[2]. According to the model by Kadomtsev[3], the unstable m = 1 tearing mode grows exponentially in time until the current profile becomes flat inside the q = 1 surface due to the magnetic field reconnection. The disruption process is reproduced in good agreement with the experimental data by a single helicity numerical calculations[4,5]. The sawtooth oscillations are recovered in a result of a tokamak code simulation based on this model modified to include the kinetic effect[6].

In the recent high-power-neutral-beam-injection experiment of the JFT-2 tokamak, it has been observed that the sawtooth oscillations are replaced by large amplitude m = 1 oscillations[7]. Although Kadomtsev's model has succeeded in the explanation of the sawtooth oscillations, it can not explain the m = 1 oscillation found in the high β_p experiments. Two possible causes of this new phenomenon are considered: (i) the mode coupling between the m = 1 and m = 2 resistive modes due to toroidicity , and (ii) the unstable m = 1 "resistive internal kink mode". In a toroidal plasma, the m = 1 and m = 2 resistive modes are coupled each other due to the outward shift of the magnetic axis. By this coupling, the magnetic energy of the m = 1 mode can be released through the m = 2 mode, and the disruption is possibly supressed. This effect becomes larger in a plasma with higher poloidal beta value because of the larger shift of the magnetic axis and of the non-uniformity of the equilibrium current density along the field line.

As for the m = 1 internal kink mode, it becomes unstable when the poloidal beta value exceeds a critical value[8]. In spite of the large growth rate, the saturation level of the mode is quite low[9,10]. The mode does not develop into the internal disruption but shows finite amplitude saturation, which is smaller than that observed in experiments. Taking into account the resistivity, the "resistive internal kink mode" develops beyond this saturation

level due to the field line reconnection. The evolution of the energy of the toroidal field works as a stabilizing factor to prevent the disruption, and the saturation of the magnetic island is expected.

The purpose of this paper is to study the effects of the toroidicity and ideal mode on the internal disruption, especially in a high beta plasma with the low q-value. In the next section we study the m = 1 internal kink mode in a tokamak by using the code ERATO and show that the internal mode becomes unstable for increasing the poloidal beta value. The unstable internal resistive mode in a cylindrical plasma is studied in §3 by using the new reduced set of the MHD equation, and the saturation of the magnetic island is shown in a plasma with the high poloidal beta value. The toroidal effects on the nonlinear evolution of the m = 1 and m = 2 tearing modes are studied in §4. Summary is given in §5.

2. Toroidal Effect on the Internal Kink Mode

In this section we study numerically the toroidal effect on the m = 1 internal kink mode by using the code THALIA[11] and the revised version of ERATO[12] which is incorporated to a high accuracy mapping module and can give accurately a solution with a small growth rate. By the numerical analysis we confirmed that the toroidicity stabilizes the internal kink mode as shown by Bussac et al.[8] and obtained some insights into the resistive internal mode.

Equilibria used in the analyses are as follows. In the toroidal calculations an FCT series of equilibria with a circular cross section and aspect ratio A of 3 is computed for a given pressure profile $p(\psi)$

$$\frac{dp}{d\psi} = p_0 [\, 1 - \alpha\psi - (1-\alpha)\psi^4 \,], \qquad 0 \leq \psi \leq 1 \tag{2.1}$$

where the parameter p_0 is varied and the safety factor profile, $q(\psi)$, is obtained for a low β and null diamagnetic current ($TdT/d\psi = 0$) equilibrium. The choice of the q-profile gives the ratio $q_a/q_0 = 2.5$. In the cylindrical case the pressure and toroidal field functions are given as

$$\frac{dp}{d\psi} = p_0 (1 - \psi) , \qquad 0 \leq \psi \leq 1 \tag{2.2}$$

$$B_z \frac{dB_z}{d\psi} = \left(\frac{1}{\beta_p} - 1\right) \frac{dp}{d\psi} . \tag{2.3}$$

level due to the field line reconnection. The evolution of the energy of the toroidal field works as a stabilizing factor to prevent the disruption, and the saturation of the magnetic island is expected.

The purpose of this paper is to study the effects of the toroidicity and ideal mode on the internal disruption, especially in a high beta plasma with the low q-value. In the next section we study the m = 1 internal kink mode in a tokamak by using the code ERATO and show that the internal mode becomes unstable for increasing the poloidal beta value. The unstable internal resistive mode in a cylindrical plasma is studied in §3 by using the new reduced set of the MHD equation, and the saturation of the magnetic island is shown in a plasma with the high poloidal beta value. The toroidal effects on the nonlinear evolution of the m = 1 and m = 2 tearing modes are studied in §4. Summary is given in §5.

2. Toroidal Effect on the Internal Kink Mode

In this section we study numerically the toroidal effect on the m = 1 internal kink mode by using the code THALIA[11] and the revised version of ERATO[12] which is incorporated to a high accuracy mapping module and can give accurately a solution with a small growth rate. By the numerical analysis we confirmed that the toroidicity stabilizes the internal kink mode as shown by Bussac et al.[8] and obtained some insights into the resistive internal mode.

Equilibria used in the analyses are as follows. In the toroidal calculations an FCT series of equilibria with a circular cross section and aspect ratio A of 3 is computed for a given pressure profile $p(\psi)$

$$\frac{dp}{d\psi} = p_0 [\, 1 - \alpha\psi - (1-\alpha)\psi^4 \,], \qquad 0 \leq \psi \leq 1 \tag{2.1}$$

where the parameter p_0 is varied and the safety factor profile, $q(\psi)$, is obtained for a low β and null diamagnetic current ($TdT/d\psi = 0$) equilibrium. The choice of the q-profile gives the ratio $q_a/q_0 = 2.5$. In the cylindrical case the pressure and toroidal field functions are given as

$$\frac{dp}{d\psi} = p_0 (1 - \psi) , \qquad 0 \leq \psi \leq 1 \tag{2.2}$$

$$B_z \frac{dB_z}{d\psi} = \left(\frac{1}{\beta_p} - 1\right) \frac{dp}{d\psi} . \tag{2.3}$$

This profile gives the ratio $q_a/q_0 \simeq 2.4$, which is the approximately same as that of the toroidal analyses. Figure 2.1 shows the profiles of the safety factor q for a toroidal (a solid line) and cylindrical (a dashed line) equilibria with $\beta_p = 1$ and $q_0 = 0.9$. The difference of the positions of the q = 1 surface is small between these two cases.
The "toroidal" wave number of the cylindrical plasma, $k_z a = na/R$, is chosen as 1/3, which corresponds to the n = 1 mode in our toroidal calculations. In Fig. 2.2 the squared growth rates Γ^2 vs. β_p are shown for $q_0 = 0.9$. The growth rate Γ^2 tends to zero for $\beta_p \to 0$ in the cylindrical model, whereas, the mode becomes stable at a finite β_p in the toroidal case. Figure 2.3 shows the stability diagram in the $q_0 - \beta_p$ plane. The solid line and the dashed line denote the stability limit for the toroidal and cylindrical cases,respectively. The dotted-solid line denotes the cylindrical equilibria where the safety factor at the plasma surface (q_a) is unity, which shows that the stability is almost determined by the existence of the q = 1 surface, in the cylindrical model. In the toroidal case, however, there is a critical β_p (β_p = 0.7 in our model) below which the internal kink mode is completely stabilized. Figure 2.4 shows the structures of the azimuthal component (ξ_θ) of the plasma displacement. As β_p decreases, ξ_θ becomes steep in the toroidal model. For $\beta_p = 0.75$, the half width of the mode is about 0.05a. When the magnetic Reynols number is $S = 10^6$, the width of the resistive layer is the order of $S^{-1/3} = 0.01$. This means that the resistivity broadens the eigenmode when $\beta_p \lesssim 0.75$. In usual ohmically heated plasmas ($\beta_p < 0.5$), the resistive mode plays a dominant role in the confinement of a plasma. When β_p increases, the width of the eigenmode is much broader than that of the resistive layer (Fig.2.4(a)) and resistive effect is weak in the exponentially growing phase.

3.Simulation of the Resistive Internal Kink Mode

In this section, we study the linear stability and the nonlinear evolution of the m = 1 "resistive internal kink mode" in a cylindrical plasma. The evolution of the tearing modes has been studied by using the usual reduced set of MHD equations. In this set of equations, however, the m = 1 internal mode is marginally stable because the driving terms of this mode, i.e., the second order terms in the inverse aspect ratio are neglected. In order to

This profile gives the ratio $q_a/q_0 \simeq 2.4$, which is the approximately same as that of the toroidal analyses. Figure 2.1 shows the profiles of the safety factor q for a toroidal (a solid line) and cylindrical (a dashed line) equilibria with $\beta_p = 1$ and $q_0 = 0.9$. The difference of the positions of the q = 1 surface is small between these two cases.
The "toroidal" wave number of the cylindrical plasma, $k_z a = na/R$, is chosen as 1/3, which corresponds to the n = 1 mode in our toroidal calculations. In Fig. 2.2 the squared growth rates Γ^2 vs. β_p are shown for $q_0 = 0.9$. The growth rate Γ^2 tends to zero for $\beta_p \to 0$ in the cylindrical model, whereas, the mode becomes stable at a finite β_p in the toroidal case. Figure 2.3 shows the stability diagram in the $q_0 - \beta_p$ plane. The solid line and the dashed line denote the stability limit for the toroidal and cylindrical cases, respectively. The dotted-solid line denotes the cylindrical equilibria where the safety factor at the plasma surface (q_a) is unity, which shows that the stability is almost determined by the existence of the q = 1 surface, in the cylindrical model. In the toroidal case, however, there is a critical β_p ($\beta_p = 0.7$ in our model) below which the internal kink mode is completely stabilized. Figure 2.4 shows the structures of the azimuthal component (ξ_θ) of the plasma displacement. As β_p decreases, ξ_θ becomes steep in the toroidal model. For $\beta_p = 0.75$, the half width of the mode is about 0.05a. When the magnetic Reynols number is $S = 10^6$, the width of the resistive layer is the order of $S^{-1/3} = 0.01$. This means that the resistivity broadens the eigenmode when $\beta_p \lesssim 0.75$. In usual ohmically heated plasmas ($\beta_p < 0.5$), the resistive mode plays a dominant role in the confinement of a plasma. When β_p increases, the width of the eigenmode is much broader than that of the resistive layer (Fig.2.4(a)) and resistive effect is weak in the exponentially growing phase.

3. Simulation of the Resistive Internal Kink Mode

In this section, we study the linear stability and the nonlinear evolution of the m = 1 "resistive internal kink mode" in a cylindrical plasma. The evolution of the tearing modes has been studied by using the usual reduced set of MHD equations. In this set of equations, however, the m = 1 internal mode is marginally stable because the driving terms of this mode, i.e., the second order terms in the inverse aspect ratio are neglected. In order to

simulate the resistive internal mode, therefore, we have to include these terms correctly.

In the following, we assume the perturbations with a single helicity ($f(\vec{r},t) = f(r,\theta+kz,t)$), the incompressible fluid motion $\nabla\cdot\vec{v} = 0$ and the uniform mass density $\rho(\vec{r},t=0) = 1$. Under these assumptions, the magnetic field $\vec{B}$ and the velocity $\vec{v}$ can be expressed by the helical flux function ψ and the helical stream function Φ as

$$\vec{B} = B_\zeta \vec{e}_h + \vec{e}_h \times \vec{\nabla}\psi \tag{3.1}$$

$$\vec{v} = v_\zeta \vec{e}_h + \vec{e}_h \times \vec{\nabla}\Phi \tag{3.2}$$

where $\vec{e}_h = (\vec{e}_\theta - kr\vec{e}_z)/\sigma$ is the unit vector along the helix and $\sigma = 1+(kr)^2$. Using these expressions, the MHD equations can be rewritten into the following equations:

$$\frac{\partial U}{\partial t} + \vec{v}\cdot\vec{\nabla}\left(U + \frac{2k}{m\sigma^2} v_\zeta\right) = \frac{k^2}{m^2\sigma^2}\frac{\partial v_\zeta^2}{\partial\theta} + \vec{B}\cdot\vec{\nabla}J - \frac{k^2}{m^2\sigma^2}\frac{\partial B_\zeta^2}{\partial\theta} \tag{3.3}$$

$$\frac{\partial v_\zeta}{\partial t} + \vec{v}\cdot\vec{\nabla}v_\zeta = \vec{B}\cdot\vec{\nabla}B_\zeta \tag{3.4}$$

$$\frac{\partial\psi}{\partial t} = \vec{B}\cdot\vec{\nabla}\Phi + \sigma\eta J - E_\zeta(t) \tag{3.5}$$

$$\frac{\partial B_\zeta}{\partial t} = -\sigma\vec{v}\cdot\vec{\nabla}\left(\frac{B_\zeta}{\sigma}\right) + \sigma\vec{B}\cdot\vec{\nabla}\left(\frac{v_\zeta}{\sigma}\right) - \frac{2k}{m\sigma}\vec{B}\cdot\vec{\nabla}\Phi + \sigma\eta R_\eta \tag{3.6}$$

$$U = \Delta^*\Phi, \quad J = \Delta^*\psi + \frac{2k}{\sigma^2}B_\zeta \text{ and } \quad R = \Delta^*B_\zeta - \frac{2k}{\sigma^2}J,$$

($m=1$), where E_ζ is the externally induced electric field, which we set such that the total plasma current is constant. The energy integral of these equations is written as

$$\frac{d}{dt}(K + M) + Q = 0 \tag{3.7}$$

where K, M and Q denote the kinetic energy, magnetic energy and the rate of the energy dissipation, respectively,

$$K = \frac{1}{2}\int\left[\frac{1}{\sigma}\left(\frac{\partial\Phi}{\partial r}\right)^2 + \left(\frac{1}{r}\frac{\partial\Phi}{\partial\theta}\right)^2 + \frac{1}{\sigma}v_\zeta^2\right]rdrd\theta \tag{3.8}$$

$$M = \frac{1}{2} \int \left[\frac{1}{\sigma} \left(\frac{\partial \psi}{\partial r}\right)^2 + \left(\frac{1}{r} \frac{\partial \psi}{\partial \theta}\right)^2 + \frac{1}{\sigma} B_\zeta{}^2\right] r dr d\theta \tag{3.9}$$

$$Q = \int \eta \left[\sigma J^2 + \frac{1}{\sigma} \left(\frac{\partial B_\zeta}{\partial r}\right)^2 + \left(\frac{1}{r} \frac{\partial B_\zeta}{\partial \theta}\right)^2\right] r dr d\theta$$

$$- \frac{r}{\sigma} \left[\left(\frac{\partial \psi}{\partial t} - E_\zeta\right) \frac{\partial \psi}{\partial r} + \eta B_\zeta \frac{\partial B_\zeta}{\partial r}\right]_{r=a} . \tag{3.10}$$

This set of equations reduces to the conventional one when the longitudinal wave number k goes to zero with keeping kB_ζ constant. Thus, the set of equations can express three different modes; i.e., the internal mode ($\eta = 0$, $k \neq 0$), tearing mode ($\eta \neq 0$, $k = 0$) and resistive internal kink mode ($\eta \neq 0$, $k \neq 0$).

Before studying the nonlinear evolution of the resistive internal kink mode, we study the parameter dependence of the linear growth rate of this mode by linearizing the equations and deriving a generalized matrix eigenvalue equation on the basis of the finite element formulation. Figure 3.1 shows the dependence of the growth rate on the longitudinal wave number k and the resistivity η, where the q profile is chosen as $q(r) = 0.9 + 0.2r^2$ and the radial mesh number N_r is $50 \sim 100$ with mesh accumulation near the $q = 1$ surface. In a cylindrical plasma, the internal mode is always unstable, except $k = 0$. When k is small and the growth rate of the tearing mode γ_η is much larger than that of the ideal mode γ_I, the localization width of the vorticity near the $q = 1$ surface is determined by the tearing mode. As k increases, the mode becomes essentially the ideal one ($\gamma_I >> \gamma_\eta$). The transition of the mode from the resistive one to the internal one is consistent with the analysis by Coppi et al.[13)]

Now we study the nonlinear evolution of the resistive internal kink mode. We Fourier-expand Eqs.(3.3) to (3.6) with respect to θ+kz. The Fourier-decomposed equations are solved by the predictor-corrector explicit time integration scheme. The evolutions of the three modes, i.e., the internal kink mode, tearing mode, and resistive internal kink mode, are studied for the same q-profile ($q(r) = 0.8(1+r^2)$) and pressure profile ($p(r) = 2(1-r^2)$). The maximum Fourier mode number is 20, and the radial mesh number is 201 with accumulation near the singular point. Figure 3.2

shows the temporal change of the position of the magnetic axis r_a for three cases. When $k = 0$ and $\eta = 10^{-4}$, the internal kink mode is marginally stable and the magnetic axis shifts outward exponentially in time due to the resistive mode, and the internal disruption occurs when the magnetic axis touches the critical surface $r = r_c$ as predicted by Kadomtsev[3]. When $k = 1/3$ and $\eta = 0$, the internal kink mode causes the shift of the magnetic axis, but this shift saturates at low level due to the development of the skin current. The saturation level of the shift $r_a \simeq 0.1$ is slightly larger than the analytic value[9]. This difference is due to the formation of a thin magnetic island caused by the numerical reason in the saturation stage.

When we take into account the finite resistivity $\eta = 10^{-4}$ (the resistive internal kink mode), the magnetic axis shifts beyond the saturation level of the internal mode due to the magnetic field line reconnection. Unlike the resistive mode, the longitudinal field B_ζ forms the island structure and the development of the large diamagnetic current prevents the further shift of the magnetic axis before it reaches the critical surface $r = r_c$. In this way, the resistive internal kink mode forms the large, saturated magnetic island. Figure 3.3 (a) shows the ψ and B_ζ contours in the saturation stage. For the comparison, the time evolution of the contours for (b) the ideal kink mode and for (c) the $m = 1$ tearing mode is also shown in the figure. These results show that the resistive internal kink mode is a candidate of the experi mentally observed large amplitude $m = 1$ oscillations.

4. Simulation of the Tearing Modes in a Toroidal Plasma

In this section we study the nonlinear evolution of the $m = 1$ mode in a low β_p toroidal plasma. In order to understand the evolution of the $m = 1$ mode in a tokamak with high poloidal beta values, we have to take into account correctly both of the mode coupling due to the toroidicity and the unstable internal kink mode. The latter effect can be neglected in a low β_p toroidal plasma. The unstable modes are only the resistive ones and it is relevant to study their evolution using the conventional set of reduced equations[14].

We consider a tokamak with circular cross section and employ the coordinates (r,θ,ϕ), where field lines are straight and $r = \sqrt{g}\, R_0/R^2$. Assuming the smallness of the inverse aspect ratio, $\varepsilon = r/R$, the reciprocal metric tensor is approximated as

$$g^{rr} = 1 + 2\frac{d\Delta}{dr}\cos\theta \; ; \quad g^{r\theta} = -\left(\frac{d^2\Delta}{dr^2} + \frac{1}{r}\frac{d\Delta}{dr} - \frac{1}{R_0}\right)\sin\theta \; ;$$

shows the temporal change of the position of the magnetic axis r_a for three cases. When $k = 0$ and $\eta = 10^{-4}$, the internal kink mode is marginally stable and the magnetic axis shifts outward exponentially in time due to the resistive mode, and the internal disruption occurs when the magnetic axis touches the critical surface $r = r_c$ as predicted by Kadomtsev[3]. When $k = 1/3$ and $\eta = 0$, the internal kink mode causes the shift of the magnetic axis, but this shift saturates at low level due to the development of the skin current. The saturation level of the shift $r_a \simeq 0.1$ is slightly larger than the analytic value[9]. This difference is due to the formation of a thin magnetic island caused by the numerical reason in the saturation stage.

When we take into account the finite resistivity $\eta = 10^{-4}$ (the resistive internal kink mode), the magnetic axis shifts beyond the saturation level of the internal mode due to the magnetic field line reconnection. Unlike the resistive mode, the longitudinal field B_ζ forms the island structure and the development of the large diamagnetic current prevents the further shift of the magnetic axis before it reaches the critical surface $r = r_c$. In this way, the resistive internal kink mode forms the large, saturated magnetic island. Figure 3.3 (a) shows the ψ and B_ζ contours in the saturation stage. For the comparison, the time evolution of the contours for (b) the ideal kink mode and for (c) the $m=1$ tearing mode is also shown in the figure. These results show that the resistive internal kink mode is a candidate of the experimentally observed large amplitude $m=1$ oscillations.

4. Simulation of the Tearing Modes in a Toroidal Plasma

In this section we study the nonlinear evolution of the $m = 1$ mode in a low β_p toroidal plasma. In order to understand the evolution of the $m = 1$ mode in a tokamak with high poloidal beta values, we have to take into account correctly both of the mode coupling due to the toroidicity and the unstable internal kink mode. The latter effect can be neglected in a low β_p toroidal plasma. The unstable modes are only the resistive ones and it is relevant to study their evolution using the conventional set of reduced equations[14].

We consider a tokamak with circular cross section and employ the coordinates (r,θ,ϕ), where field lines are straight and $r = \sqrt{g}\, R_0/R^2$. Assuming the smallness of the inverse aspect ratio, $\varepsilon = r/R$, the reciprocal metric tensor is approximated as

$$g^{rr} = 1 + 2\frac{d\Delta}{dr}\cos\theta \; ; \quad g^{r\theta} = -\left(\frac{d^2\Delta}{dr^2} + \frac{1}{r}\frac{d\Delta}{dr} - \frac{1}{R_0}\right)\sin\theta \; ;$$

$$g^{\theta\theta} = \frac{1}{r^2}\{1 - 2(\frac{d\Delta}{dr} - \frac{r}{R})\cos\theta\}; \qquad g^{\phi\phi} = R_0^2(1 + 2\frac{r}{R_0}\cos\theta), \tag{4.1}$$

where Δ is the shift of the magnetic axis defined by

$$\Delta(r) = \frac{1}{R_0}\int_r^a \frac{dr}{rB_\theta^2}\int_0^r (B_\theta^2 - 2r\frac{dp}{dr})rdr. \tag{4.2}$$

The safety factor and pressure profiles used in the following simulations are; $q(r) = 0.9\{1-(r/r_0)^{2\lambda}\}^{1/\lambda}$ with $r_0 = 0.5$ and $\lambda = 2 + 2r^2$, and $p(r) = p_0(1-r^2)^2$. We employ the equal spacing radial meshes ($N_r = 201$), the maximum mode number $M_m = 31$ and the implicit-explicit time integration scheme.

Figure 4.1 shows the temporal evolution of the magnetic islands with different helicity for the aspect ratio $R_0/a = 10$, the poloidal beta value $\beta_p = 0$ and the resistivity $\eta = 10^{-4}$. The phase of the initial perturbation of the m=2/n=1 mode is chosen to be the same as that of the m = 1 mode for the case (a) and opposite for the case (b). For the comparison, the cylindrical case ($R_0/a = \infty$) is also subject to the simulation (case (c)). The behavior of the m = 1 mode in a toroidal plasma is essentially the same as in the cylindrical plasma. Untill the m = 1 mode grows to a finite level ($t < 50$), the m = 2 magnetic island also grows independently of the m = 1 mode as in the cylindrical plasma. Thereafter, the m = 2 mode is strongly affected by the m = 1 mode through the toroidal coupling. For the case (a), the m = 2 island shrinks and finally changes its phase. On the other hand, the island width for the case (b) is widened by the toroidal effect. This can be seen more remarkably in Fig. 4.2, where the evolution of the magnetic energies with the different helicity is plotted. The energy of the m = 2 mode with the initially opposite phase grows exponentially with the growth rate of about half of that of the m = 1 mode without entering the Rutherford regime, while the energy of the m = 2 mode for the case (a) decreases from the one for the cylindrical case.

Now we consider the difference of the toroidal effect on the m = 2 modes of the in-phase and opposite-phase cases. The total energy of the reduced set of MHD equations in a toroidal plasma is given by

$$E = \frac{1}{2}\int_0^a [\,(\frac{R}{R_0})^2 |\nabla\Phi|^2 + (\frac{R_0}{R})^2 |\nabla\psi|^2\,]\, d\tau \tag{4.3}$$

This energy can be devided into two parts; the cylindrical energy, E_{cyl}, and

the toroidal one, E_{tor}. When we divide the reciprocal metric g^{ij} into the cylindrical one $\bar{g}^{ij}$ and the toroidal one $\tilde{g}^{ij}(\theta)$, then E_{tor} is expressed, up to the first order of ε, as

$$E_{tor} = \int_0^a [\{\tilde{g}^{ij}(\theta) + \tilde{g}^{ij}(-\theta)\}\left(\frac{\partial\Phi_1}{\partial x^i}\frac{\partial\Phi_2}{\partial x^j} + \frac{\partial\psi_1}{\partial x^i}\frac{\partial\psi_2}{\partial x^j}\right) - \frac{4r}{R_0}\bar{g}^{ii}\frac{\partial\Phi_1}{\partial x^i}\frac{\partial\Phi_2}{\partial x^i}]d\tau \quad (4.4)$$

where we take into account only the toroidal coupling between the $m=1$ (the suffix "1") and $m=2$ (the suffix "2") modes. We approximate Φ_1 and Φ_2 as $\Phi_1 \simeq \hat{\Phi}_1 r/r_{s|m=1}$ and $\Phi_2 \simeq \hat{\Phi}_2\{r/r_{s|m=1}\}^2$ in the region $r \leq r_{s|m=1}$. Then using the relation $\psi_m = -F_m\Phi_m/\gamma_m$, we have

$$E_{tor} \simeq \frac{4}{R_0}\int_0^{r_{s|m=1}} dr(\psi_1\psi_2 - 3\Phi_1\Phi_2) \simeq \frac{4}{R_0}\int_0^{r_{s|m=1}} dr\ \psi_1\psi_2 , \quad (4.5)$$

where γ_m is the growth rate of each mode and $F_m = mB_\theta/r + nB_z/R_0$. This expression shows that the sign of the toroidal coupling energy E_{tor} depends on the phase between the $m=1$ and $m=2$ modes. Because of the small dissipation, the total energy of the system is almost conserved, so that E_{cyl} becomes smaller (or greater) than that in the cylindrical plasma for $\psi_1\psi_2 > 0$ (or $\psi_1\psi_2 < 0$). Since the $m=1$ mode has the larger growth rate and the larger amplitude than those of the $m=2$ mode, the effect of the toroidal coupling on the $m=1$ mode can be neglected. Therefore, the energy of the $m=2$ mode decreases (or increases) due to the toroidal coupling for $\psi_1\psi_2 > 0$ (or $\psi_1\psi_2 < 0$). From these results we see that the toroidal coupling influences only on the $m=2$ mode; the evolution of the $m=1$ mode is almost unaffected and the disruption occurs after the same development shown in the cylindrical calculations.

5. Conclusion

In this paper, we have studied the linear stability and the nonlinear evolution of the $m=1$ mode. The results obtained here are summarized as the followings;

1. By using the revised version of the code ERATO, it was confirmed that the toroidicity has the stabilizing effect on the $m=1$ internal kink mode and the mode is unstable only for the polidal beta higher than a critical value in a toroidal plasma.

the toroidal one, E_{tor}. When we divide the reciprocal metric g^{ij} into the cylindrical one $\bar{g}^{ij}$ and the toroidal one $\tilde{g}^{ij}(\theta)$, then E_{tor} is expressed, up to the first order of ε, as

$$E_{tor} = \int_0^a [\{\tilde{g}^{ij}(\theta) + \tilde{g}^{ij}(-\theta)\}\left(\frac{\partial\Phi_1}{\partial x^i}\frac{\partial\Phi_2}{\partial x^j} + \frac{\partial\psi_1}{\partial x^i}\frac{\partial\psi_2}{\partial x^j}\right) - \frac{4r}{R_0}\bar{g}^{ii}\frac{\partial\Phi_1}{\partial x^i}\frac{\partial\Phi_2}{\partial x^i}]d\tau \quad (4.4)$$

where we take into account only the toroidal coupling between the $m = 1$ (the suffix "1") and $m = 2$ (the suffix "2") modes. We approximate Φ_1 and Φ_2 as $\Phi_1 \simeq \hat{\Phi}_1 r/r_{s|m=1}$ and $\Phi_2 \simeq \hat{\Phi}_2\{r/r_{s|m=1}\}^2$ in the region $r \leq r_{s|m=1}$. Then using the relation $\psi_m = -F_m\Phi_m/\gamma_m$, we have

$$E_{tor} \simeq \frac{4}{R_0}\int_0^{r_{s|m=1}} dr(\psi_1\psi_2 - 3\Phi_1\Phi_2) \simeq \frac{4}{R_0}\int_0^{r_{s|m=1}} dr\ \psi_1\psi_2 , \quad (4.5)$$

where γ_m is the growth rate of each mode and $F_m = mB_\theta/r + nB_z/R_0$. This expression shows that the sign of the toroidal coupling energy E_{tor} depends on the phase between the $m = 1$ and $m = 2$ modes. Because of the small dissipation, the total energy of the system is almost conserved, so that E_{cyl} becomes smaller (or greater) than that in the cylindrical plasma for $\psi_1\psi_2 > 0$ (or $\psi_1\psi_2 < 0$). Since the $m = 1$ mode has the larger growth rate and the larger amplitude than those of the $m = 2$ mode, the effect of the toroidal coupling on the $m = 1$ mode can be neglected. Therefore, the energy of the $m = 2$ mode decreases (or increases) due to the toroidal coupling for $\psi_1\psi_2 > 0$ (or $\psi_1\psi_2 < 0$). From these results we see that the toroidal coupling influences only on the $m = 2$ mode; the evolution of the $m = 1$ mode is almost unaffected and the disruption occurs after the same development shown in the cylindrical calculations.

5. Conclusion

In this paper, we have studied the linear stability and the nonlinear evolution of the $m = 1$ mode. The results obtained here are summarized as the followings;

1. By using the revised version of the code ERATO, it was confirmed that the toroidicity has the stabilizing effect on the $m = 1$ internal kink mode and the mode is unstable only for the polidal beta higher than a critical value in a toroidal plasma.

2. The nonlinear evolution of the resistive internal kink mode in a cylindrical plasma shows that the internal disruption can be suppressed due to the modulation of the longitudinal field.
3. In a low β toroidal plasma with large aspect ratio, the behaviour of the m = 1 tearing mode is found to be essentially the same as in a cylindrical plasma. The m = 2 tearing mode, however, suffers a strong effect of the m = 1 mode through the toroidal coupling and forms the magnetic island with larger width than in a cylindrical case.

All these results show that the Kadomtsev's model of the internal disruption is valid in a toroidal plasma with the low poloidal beta. In a high β plasma,however,the internal kink mode was shown to be unstable and this mode plays an important role on the evolution of the m = 1 mode. Although the simulation of the nonlinear evolution of the resistive internal kink mode has been studied only in a cylindrical plasma, we can expect the saturation of the island in a toroidal plasma. As for the simulation of the tearing modes in a toroidal plasma, we could not see the remarkable change of the m = 1 mode for $\beta_p = 0$. We also simulated the case with $\beta_p = 1$, and the result is the same as for $\beta_p = 0$. The reason is considered to be that the pressure driven term was dropped in the simulation. The effect of this term is now under investigation.

In order to extend these results and to understand the saturation of the m = 1 mode observed in the high β tokamk experiments, we are preparing the simulation which includes both effects of the unstable internal kink mode and the toroidicity.

Acknowledgments

The authors would like to thank Dr. M. Tanaka for his helpful discussion and continuing encouragement throughout the whole work. It is also a pleasure to thank Dr. Y. Obata for his encouragement during the whole work. They are grateful to Dr. T. Matsuura for the collaboration concerning vectorization of the numerical codes. Members of the experiment group are greatly acknowledged for the fruitful discussion about the results of the high-power-neutral-beam-injection experiment in the JFT-2 tokamak.

2. The nonlinear evolution of the resistive internal kink mode in a cylindrical plasma shows that the internal disruption can be suppressed due to the modulation of the longitudinal field.
3. In a low β toroidal plasma with large aspect ratio, the behaviour of the m = 1 tearing mode is found to be essentially the same as in a cylindrical plasma. The m = 2 tearing mode, however, suffers a strong effect of the m = 1 mode through the toroidal coupling and forms the magnetic island with larger width than in a cylindrical case.

All these results show that the Kadomtsev's model of the internal disruption is valid in a toroidal plasma with the low poloidal beta. In a high β plasma,however,the internal kink mode was shown to be unstable and this mode plays an important role on the evolution of the m = 1 mode. Although the simulation of the nonlinear evolution of the resistive internal kink mode has been studied only in a cylindrical plasma, we can expect the saturation of the island in a toroidal plasma. As for the simulation of the tearing modes in a toroidal plasma, we could not see the remarkable change of the m = 1 mode for $\beta_p = 0$. We also simulated the case with $\beta_p = 1$, and the result is the same as for $\beta_p = 0$. The reason is considered to be that the pressure driven term was dropped in the simulation. The effect of this term is now under investigation.

In order to extend these results and to understand the saturation of the m = 1 mode observed in the high β tokamk experiments, we are preparing the simulation which includes both effects of the unstable internal kink mode and the toroidicity.

Acknowledgments

The authors would like to thank Dr. M. Tanaka for his helpful discussion and continuing encouragement throughout the whole work. It is also a pleasure to thank Dr. Y. Obata for his encouragement during the whole work. They are grateful to Dr. T. Matsuura for the collaboration concerning vectorization of the numerical codes. Members of the experiment group are greatly acknowledged for the fruitful discussion about the results of the high-power-neutral-beam-injection experiment in the JFT-2 tokamak.

References

1) S. von Goeler, W. Stodiek and N. Sauthoff, Phys. Rev. Lett. 33 (1974) 1201.
2) DIVA Group, Nucl. Fusion 20 (1980) 271.
3) B. B. Kadomtsev, Fizika Plasmy 1 (1975) 710.
4) B.V.Waddel et al., Nucl. Fusion 16 (1976) 528.
5) A.F.Danilov et al., Fizika Plasmy 2 (1976) 167.
6) M. Okamoto, private communication.
7) S. Yamamoto et al., Nucl. Fusion 21 (1981) 993.
8) M. N. Bussac et al., Phys. Rev. Lett. 35 (1975) 1638
9) M. N. Rosenbluth, R. Y. Dagazian and P. H. Rutherford, Phys. Fluids 16 (1973) 1894.
10) W. Park et al., Nucl Fusion 20 (1980) 1181.
11) K. Appart et al., Comput. Phys. Commn. 10 (1975) 11.
12) S. Tokuda et al., in preparation. The original version of ERATO is published by R. Gruber et al. in Compt. Phys. Commn. 21 (1981) 323.
13) B. Coppi et al., Sov. J. Plasma Phys. 2 (1976) 533.
14) G. Kurita et al., "Major disruption process in a tokamak", JAERI-M 9788 (1981).

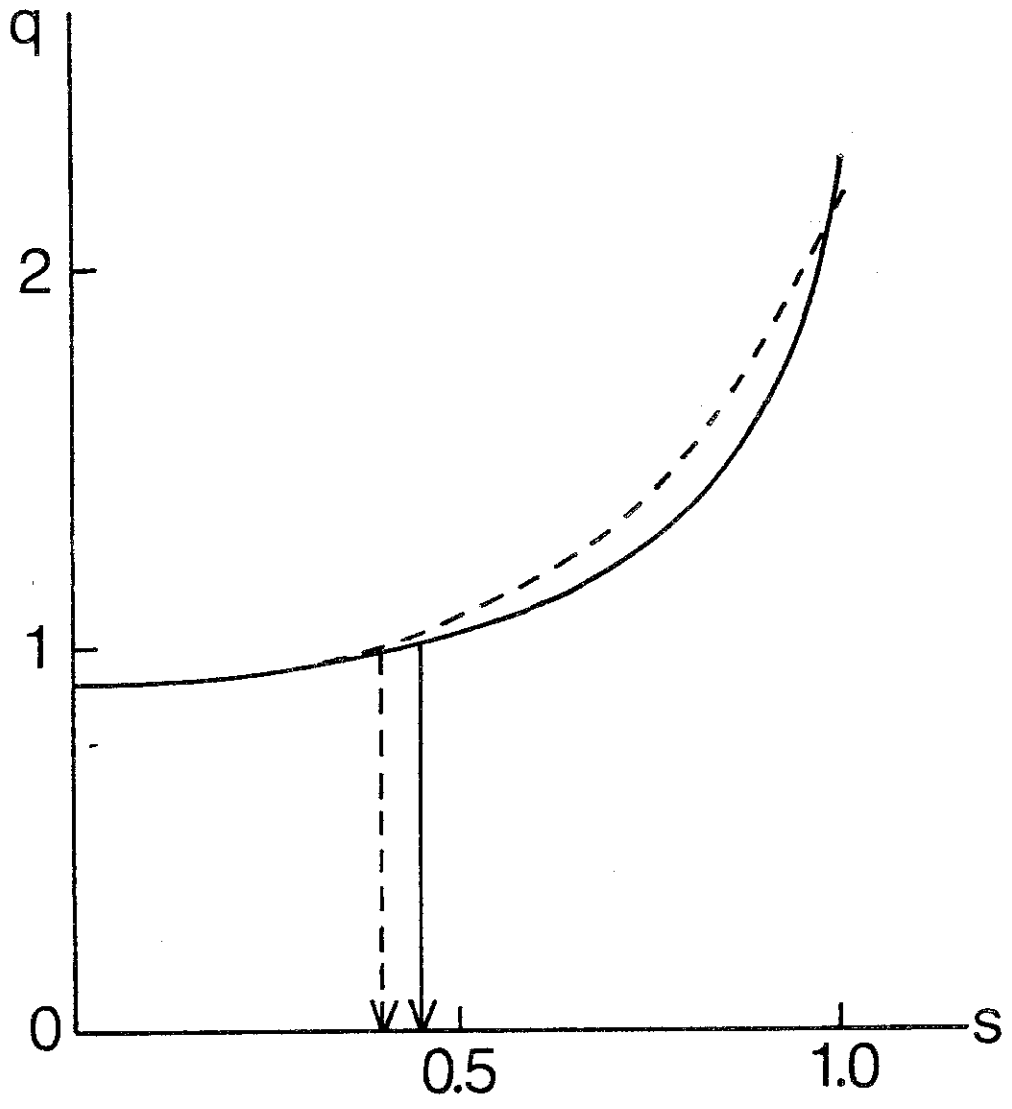

Fig.2.1 Profiles of safety factor q(s) ($s = \sqrt{\psi/\psi_s}$) for $\beta_p = 1$ and $q_0 = 0.9$. The solid and dashed lines denote the toroidal and cylindrical cases, respectively. The q = 1 surfaceses lie at s = 0.45 (the toroidal case) and s = 0.4 (the cylindrical case).

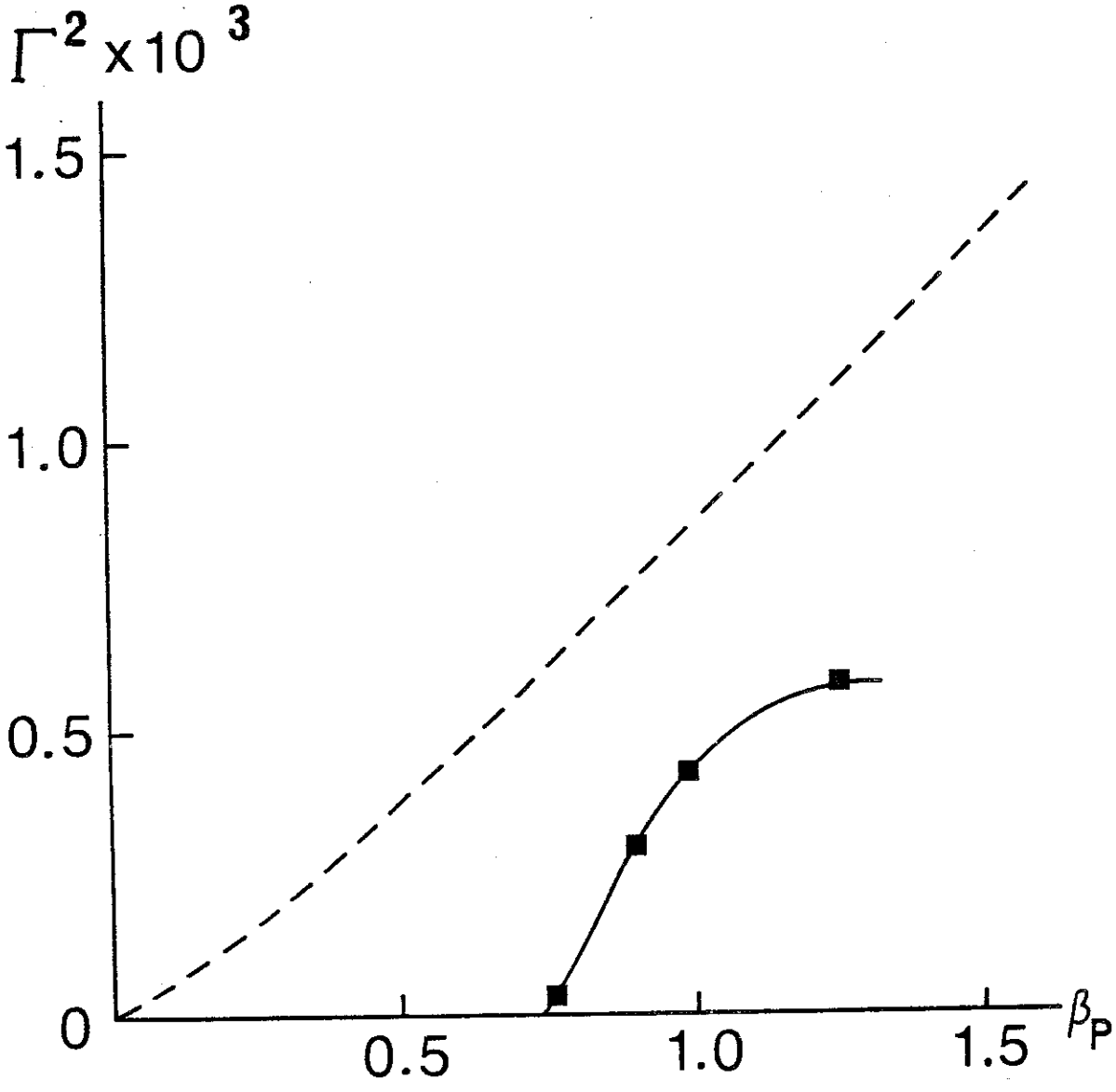

Fig.2.2 Squared growth rate Γ^2.vs. β_p for $q_0 = 0.9$. The growth rate tends to zero for $\beta_p \to 0$ in the cylindrical case (dotted line), whereas the mode becomes stable at a finite β_p ($\beta_p = 0.7$) in the toroidal case (solid line).

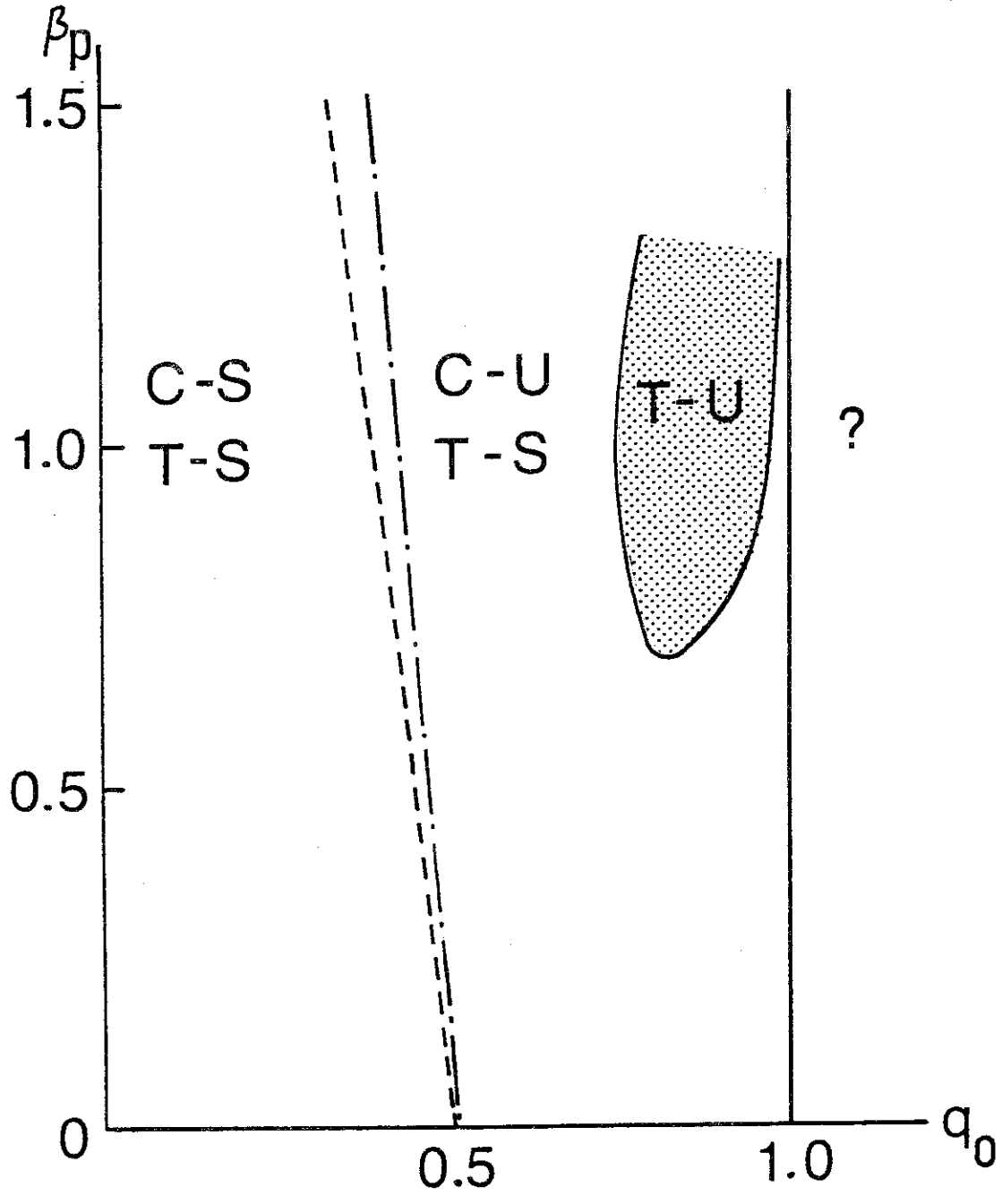

Fig.2.3 Stability diagram in the q_0- β_p plane. The stability limit for the cylindrical case (dashed line) is almost determined by the existence of the q = 1 surface (dotted-solid line). In the toroidal case, there is a critical β_p (β_p = 0.7) in the stability limit (solid line) below which the internal kink mode is stabilized.

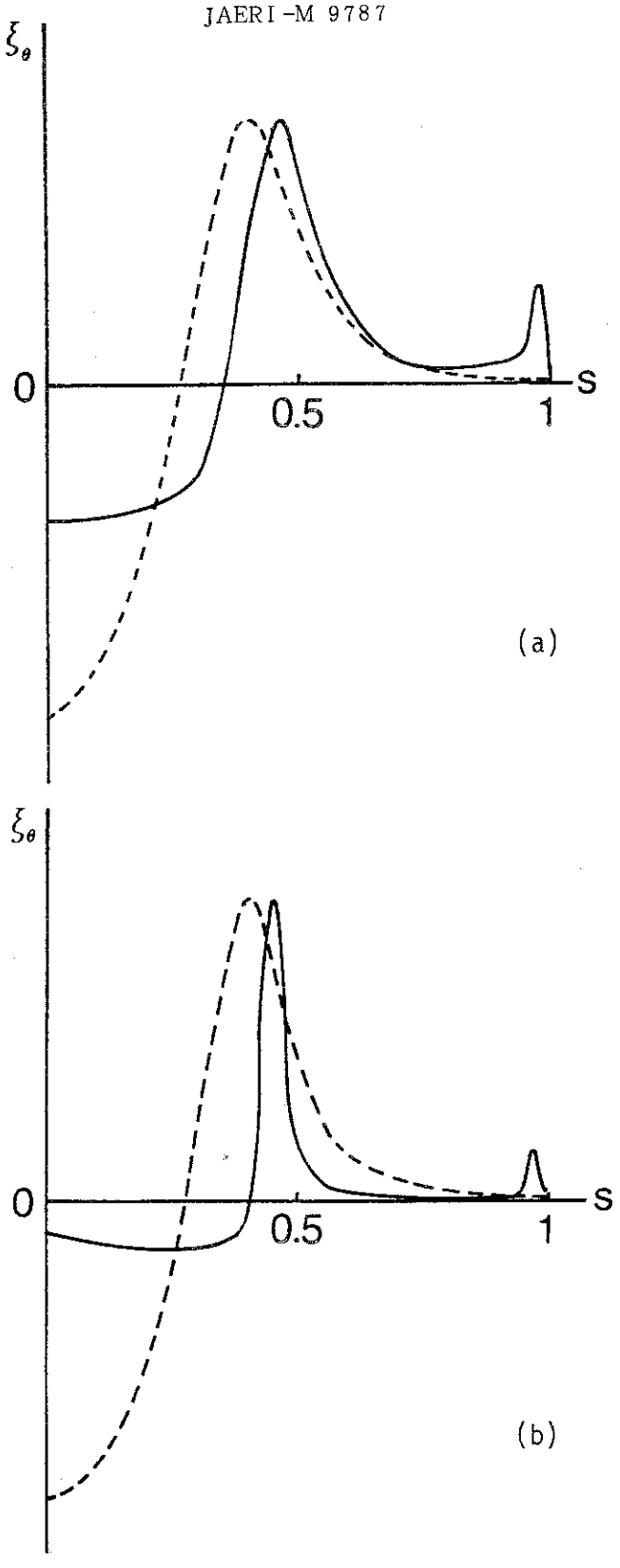

Fig.2.4 Structures of the azimuthal component (ξ_θ) of the plasma displacement for (a) β_p = 1.25 and (b) β_p = 0.75. The solid line denotes the toroidal case and the dashed line the cylindrical case. As β_p decreases, ξ_θ becomes steep for the toroidal case and the half width of the mode at q = 1 surface for β_p = 0.75 is comparable to that of the resistive layer $S^{-1/3}$ = 0.01 for $S = 10^6$.

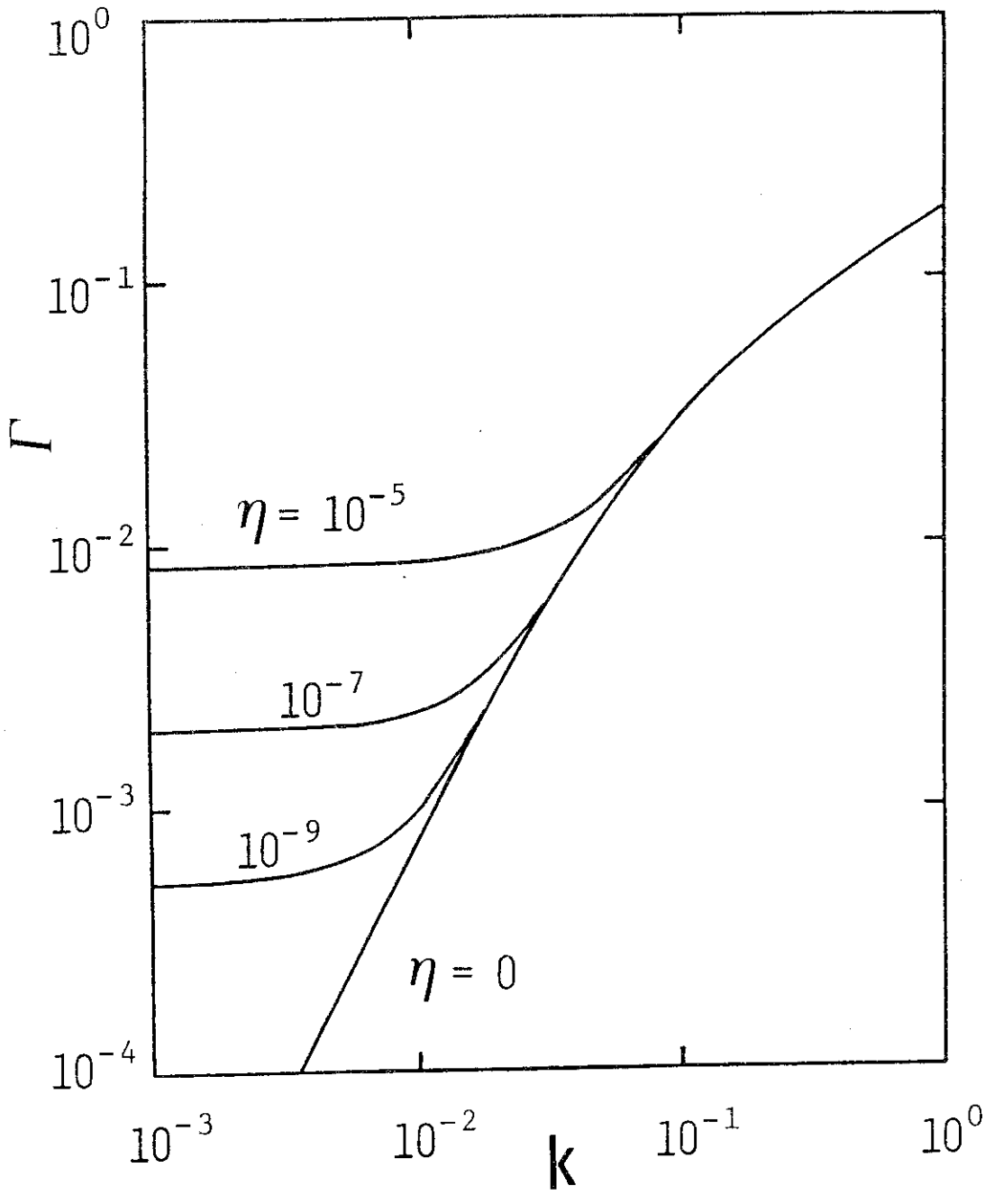

Fig.3.1 Dependence of the linear growth rate Γ of the resistive internal kink mode on the longitudinal wave number k . The safety factor profile is $q(r) = 0.9 + 0.2r^2$.

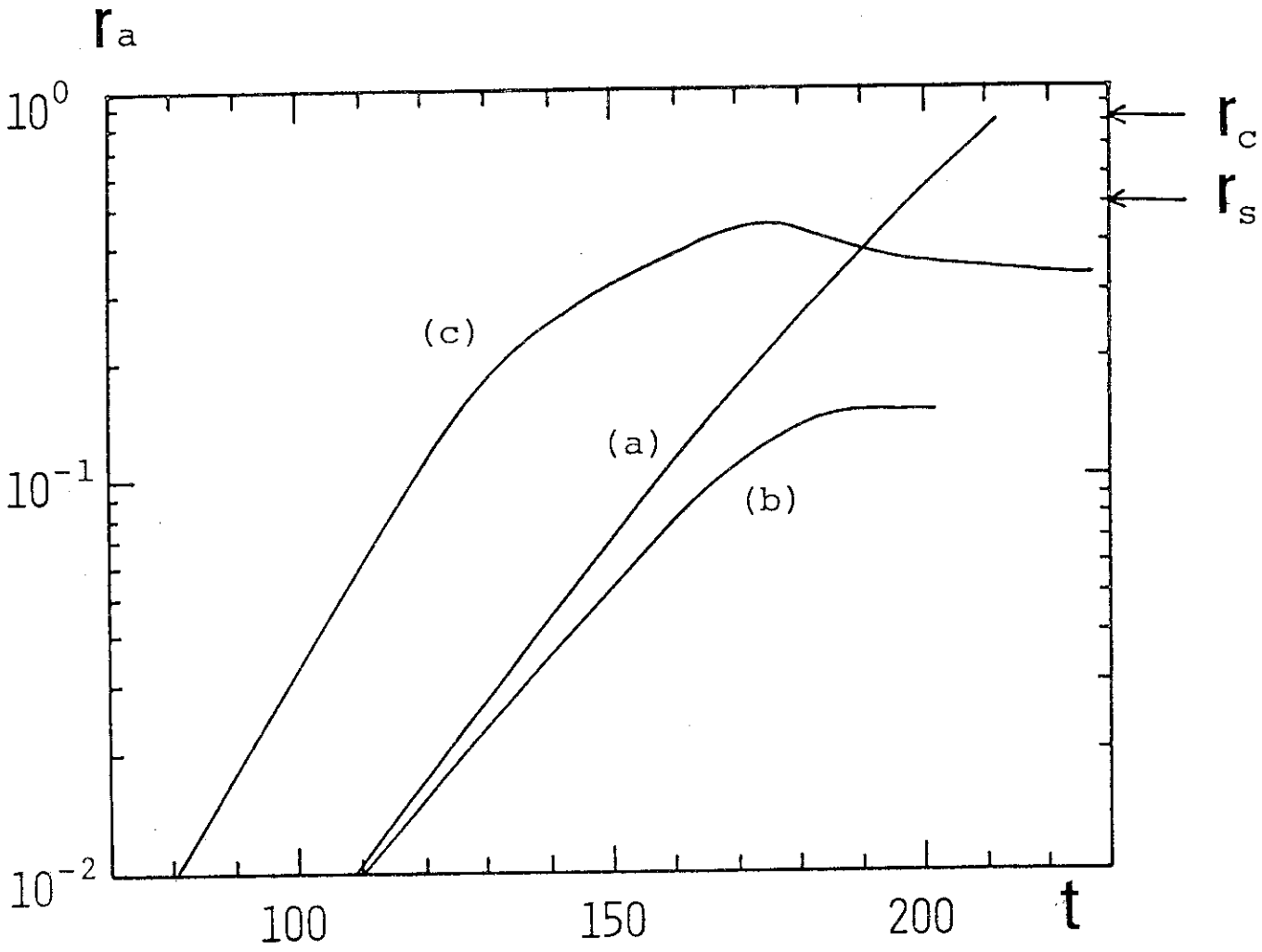

Fig.3.2 Evolution of the magnetic axis due to (a) the tearing mode ($\eta = 10^{-4}, k = 0$), (b) the internal kink mode ($\eta = 0$, $k = 1/3$), and (c) the resistive internal kink mode ($\eta = 10^{-4}$, $k = 1/3$). The profiles of the safety factor and the pressure are $q(r) = 0.8(1 + r^2)$ and $p(r) = 2(1 - r^2)$, respectively. The positions of the rational surface and of the critical surface for the disruption are denoted by 'r_s' and 'r_c', respectively.

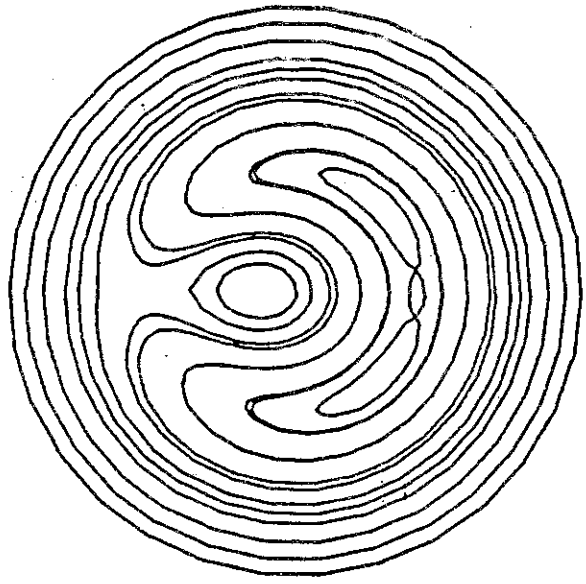

ψ-contour

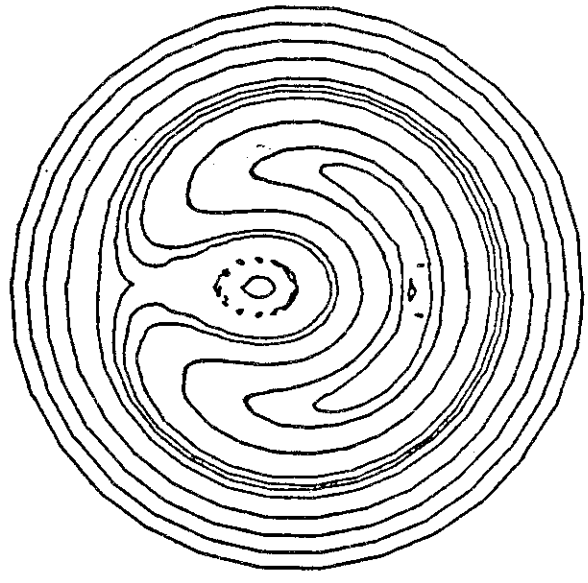

B_ζ-contour

Fig.3.3 (a)Contour of ψ and B_ζ at the saturation stage of the resistive internal kink mode.

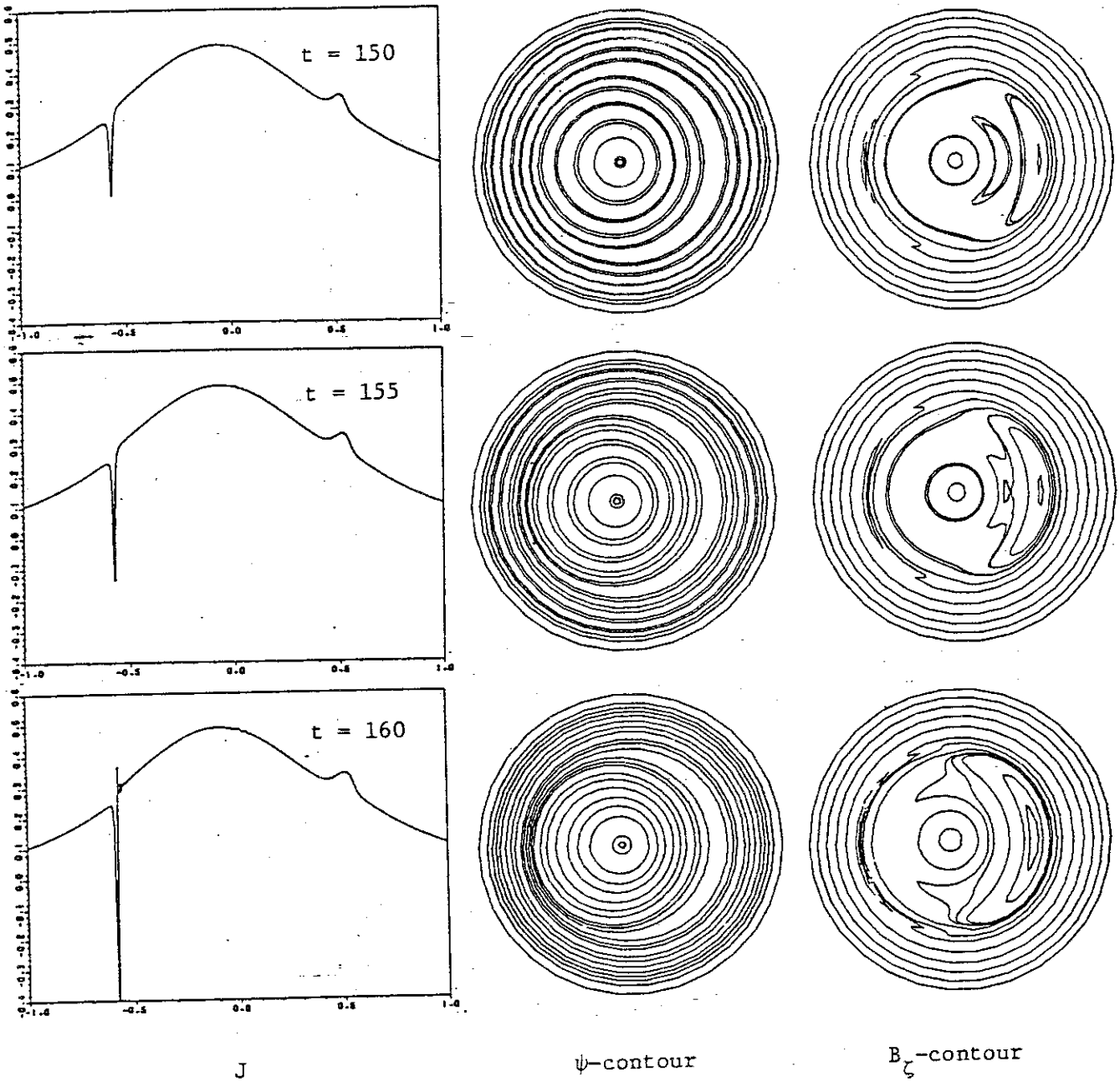

Fig3.3 (b)Time evolution of the toroidal current density, helical magnetic flux and toroidal magnetic field for the internal kink mode. The sharp peak of the toroidal current develops at r≈0.6. The rational surface is r_s=0.5.

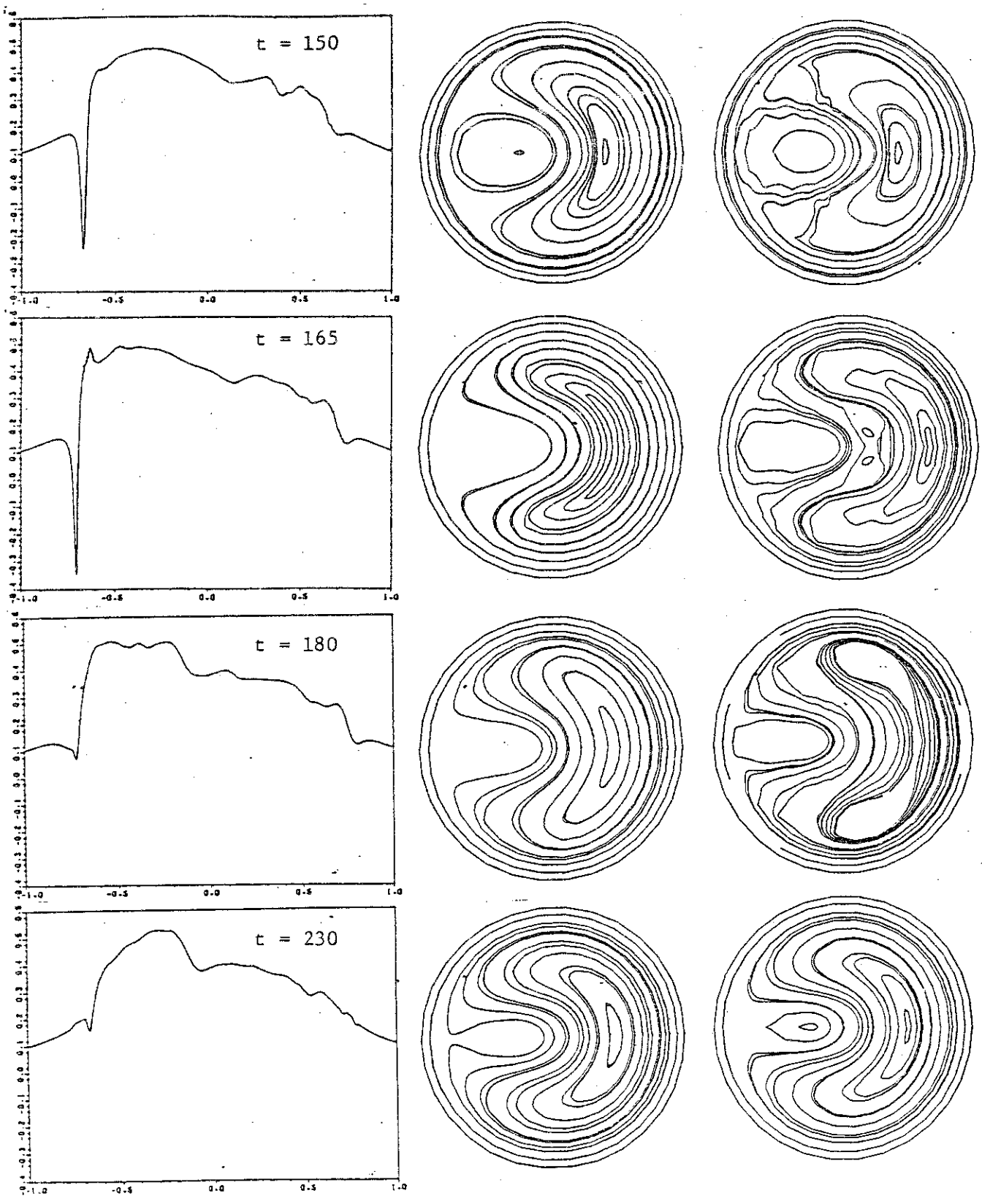

Fig3.3(c)Time evolution of the toroidal current density, helical magnetic flux and toroidal magnetic field. The sharp peak of the current disappears at t=180, and the large magetic island appears at t=230.

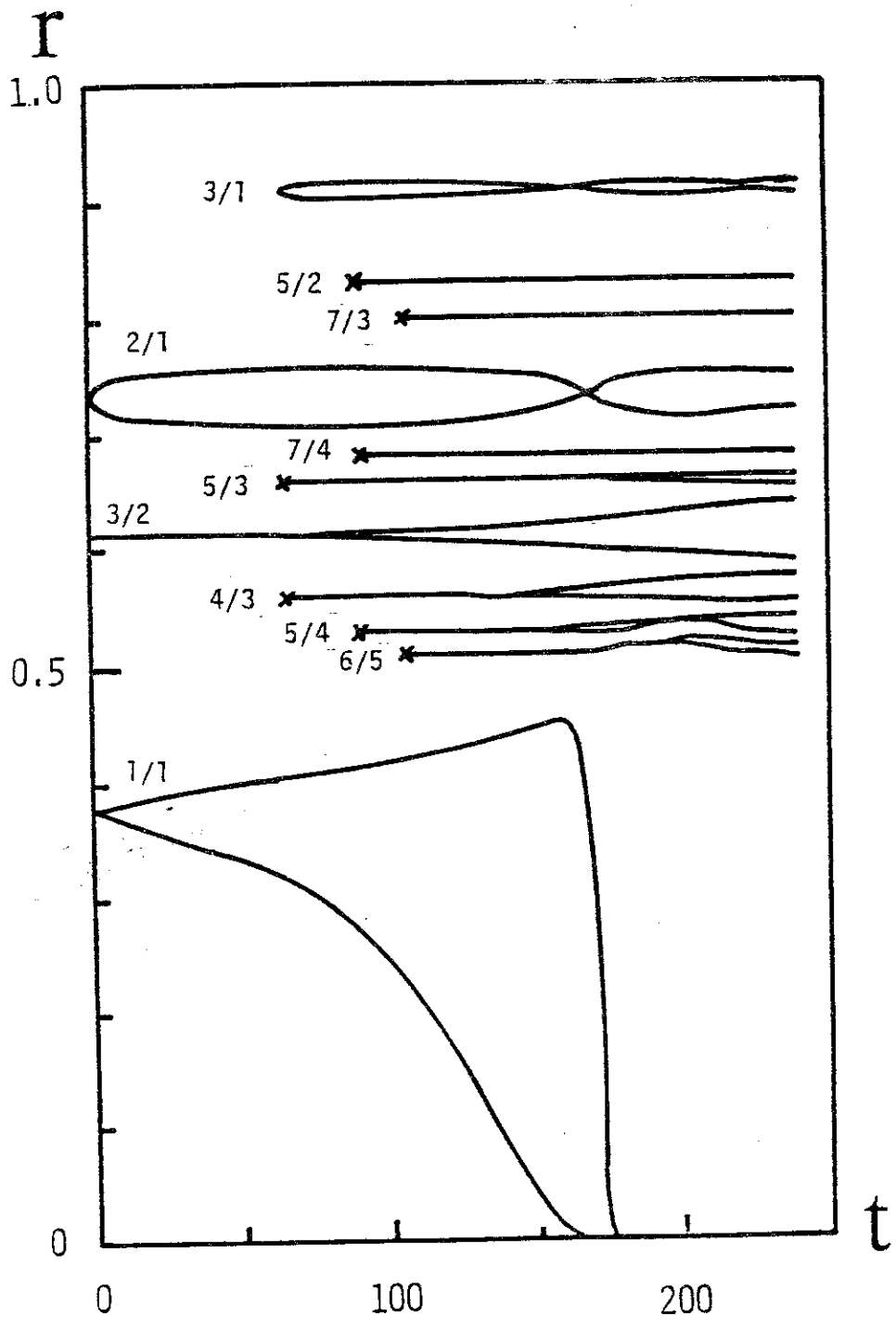

Fig.4.1 (a) Evolution of the magnetic islands with different helicity m/n for the case that the initial phase of the m = 2 mode is the same as that of the m = 1 mode. The mode number m and n denote the poloidal and toroidal ones, respectively. The safety factor is $q(r) = 0.9\ (1-(r/0.5)^{2\lambda})^{1/\lambda}$ with $\lambda = 2 + 2r^2$ and the aspect ratio is 10. The internal disruption occurs at $t \simeq 160$.

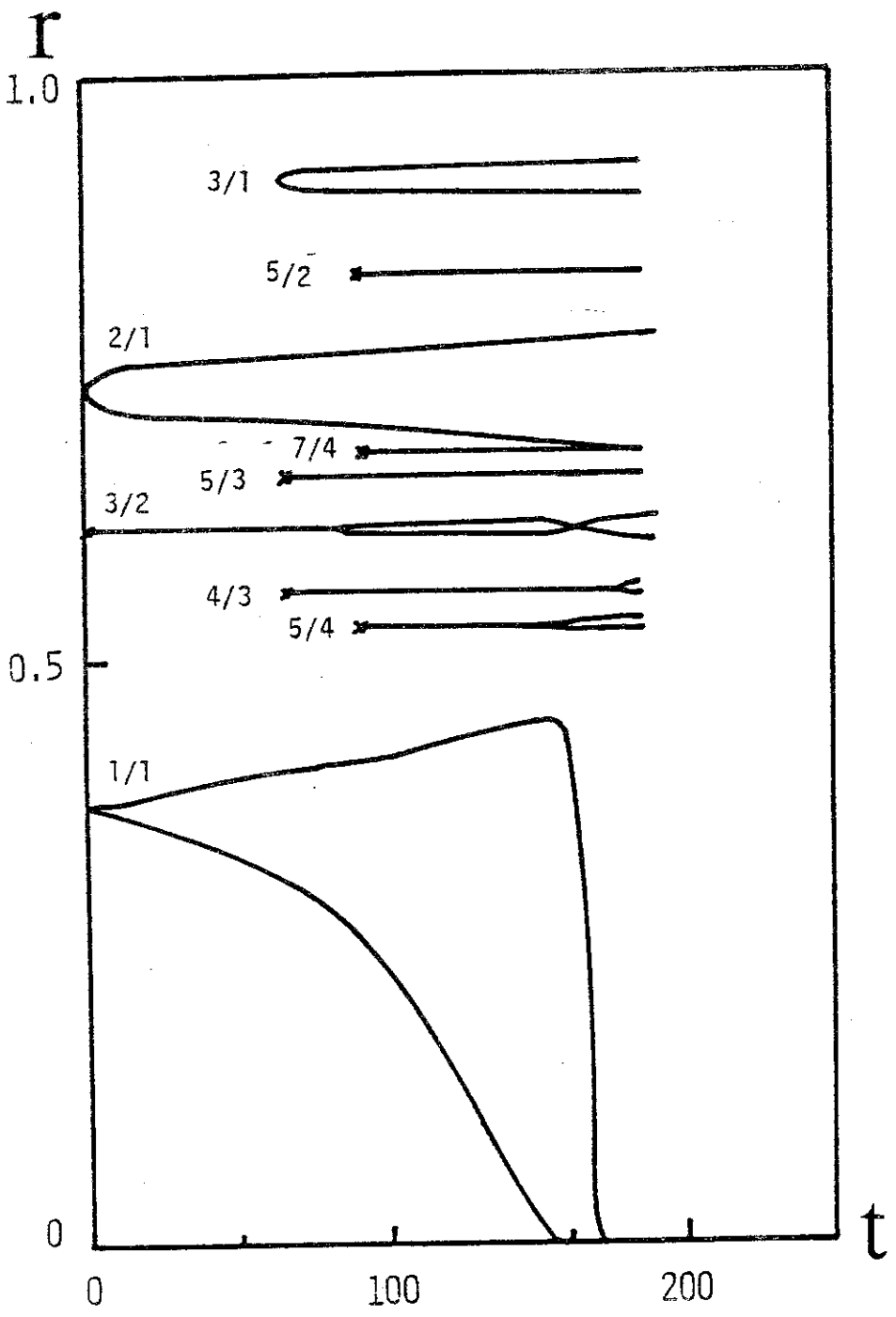

Fig.4.1 (b) Evolution of the m/n magnetic islands for the case that the initial phase of the m=2 mode is opposite to that of the m=1 mode. Other parameters are the same as those for Fig.4.1 (a). The internal disruption occurs at t $\simeq$ 160 as in Fig.4.1 (a).

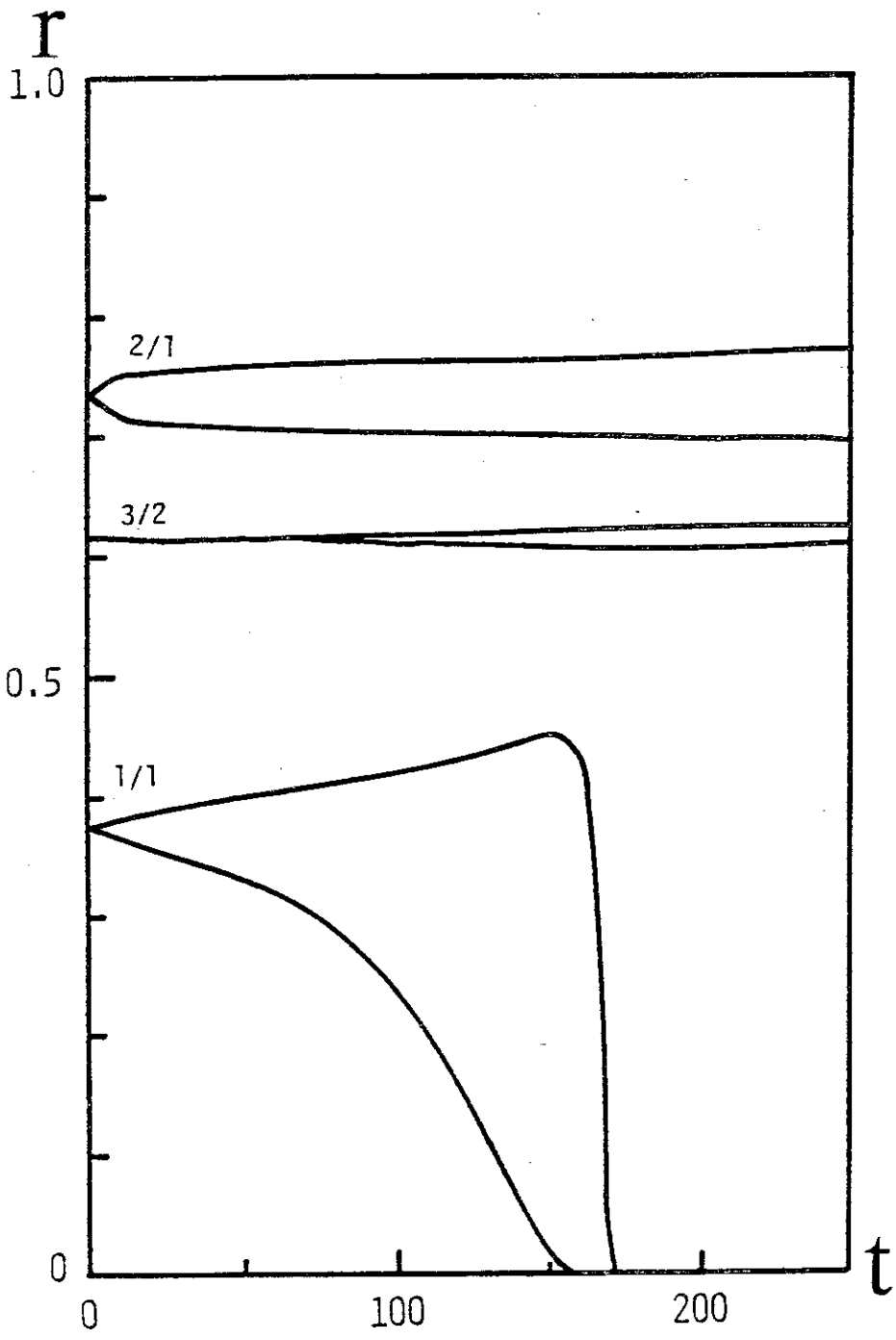

Fig.4.1 (c) Evolution of the m/n magnetic islands in a cylindrical plasma with the q-profile $q(r) = 0.9\,(1-(r/0.5)^{2\lambda})^{1/\lambda}$ $(\lambda = 2 + 2r^2)$. The internal disruption occurs at $t \simeq 160$ as in Figs.4.1 (a) and (b). The width of the 2/1 magnetic island lies between those in Fig.4.1 (a) and in Fig.4.1 (b).

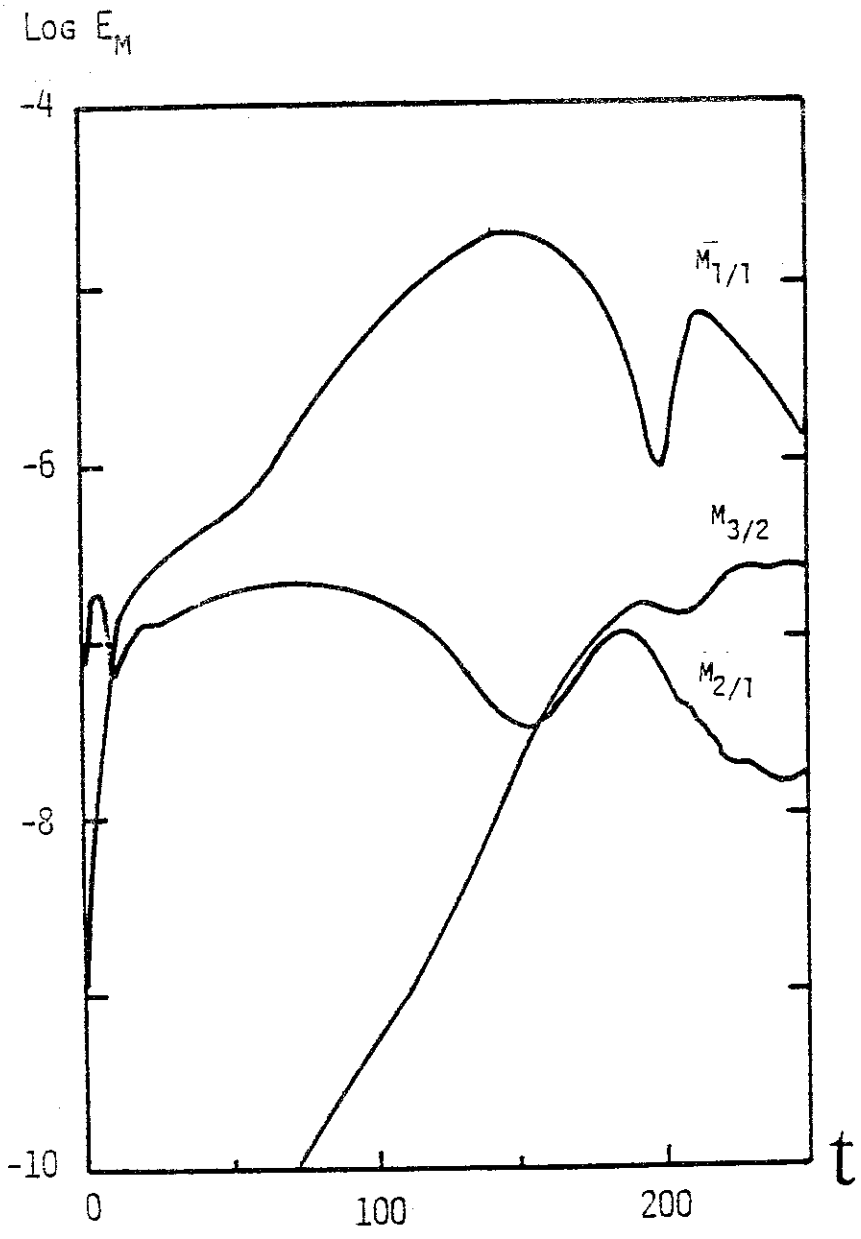

Fig.4.2 (a) Evolution of the magnetic energy defined by

$$M_{m/n} = \frac{1}{2}\int \left[\left(\frac{\partial \psi_{m/n}}{\partial r}\right)^2 + \left(\frac{m}{r}\psi_{m/n}\right)^2\right] r\,dr$$

with different helicity (m/n = 1/1, 2/1 and 3/2) for the case that the initial phase of the m = 2 mode is the same as that of the m = 1 mode. Other parameters are the same as those for Fig. 4.1. The toroidal effect on the magnetic energy of the m = 2 mode appears earlier than that on the magnetic island. The width of the island is determined by the perturbation at the rational surface. The m = 1 perturbation is restricted within it's critical radius $r_c \simeq \sqrt{2}\, r_{s|m=1}$, so that the toroidal effect of this mode on the m = 2 mode is also restricted within this radius. The m = 2 perturbation in $r < r_c$ propagates to the rational surface $r_{s|m=2}$ after a while.

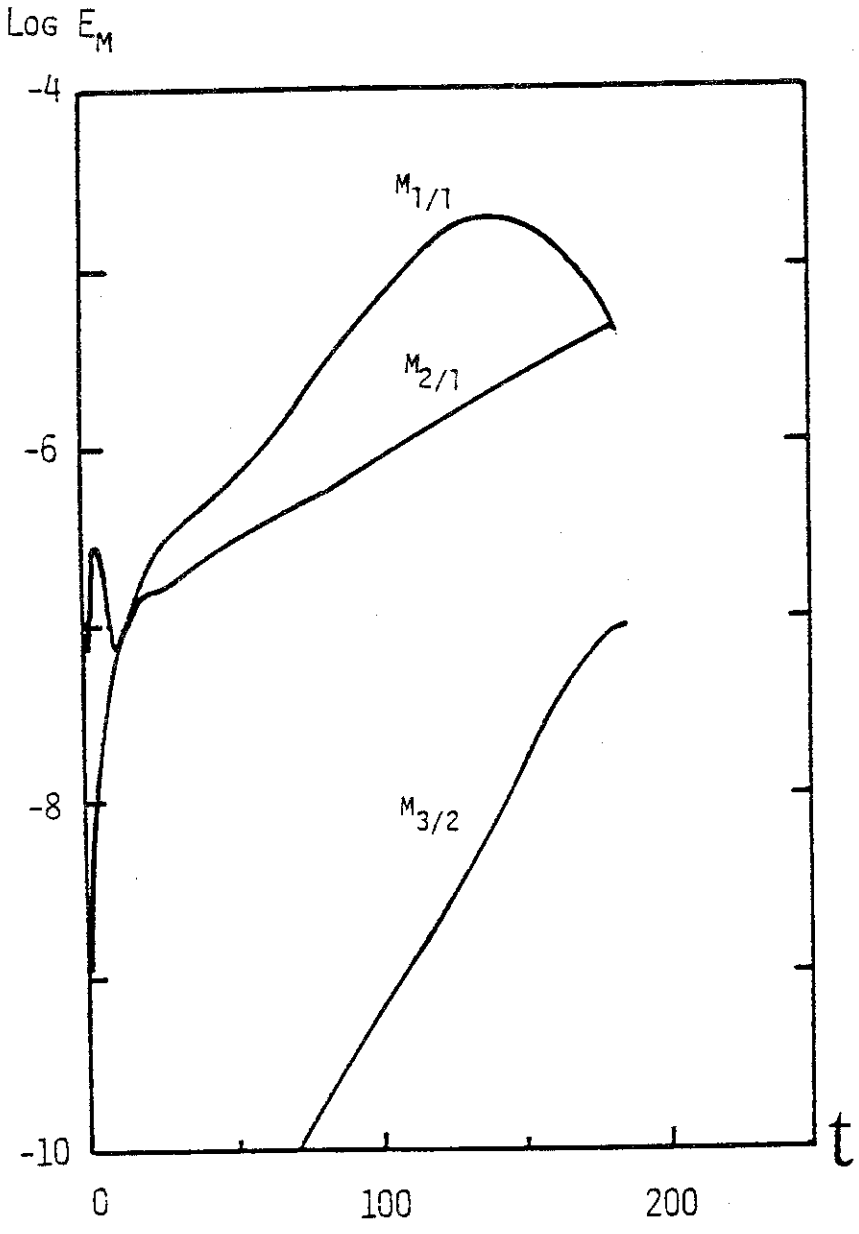

Fig.4.2 (b) Evolution of the m/n mode magnetic energy for the case that the initial phase of the m = 2 mode is opposite to that of the m = 1 mode.

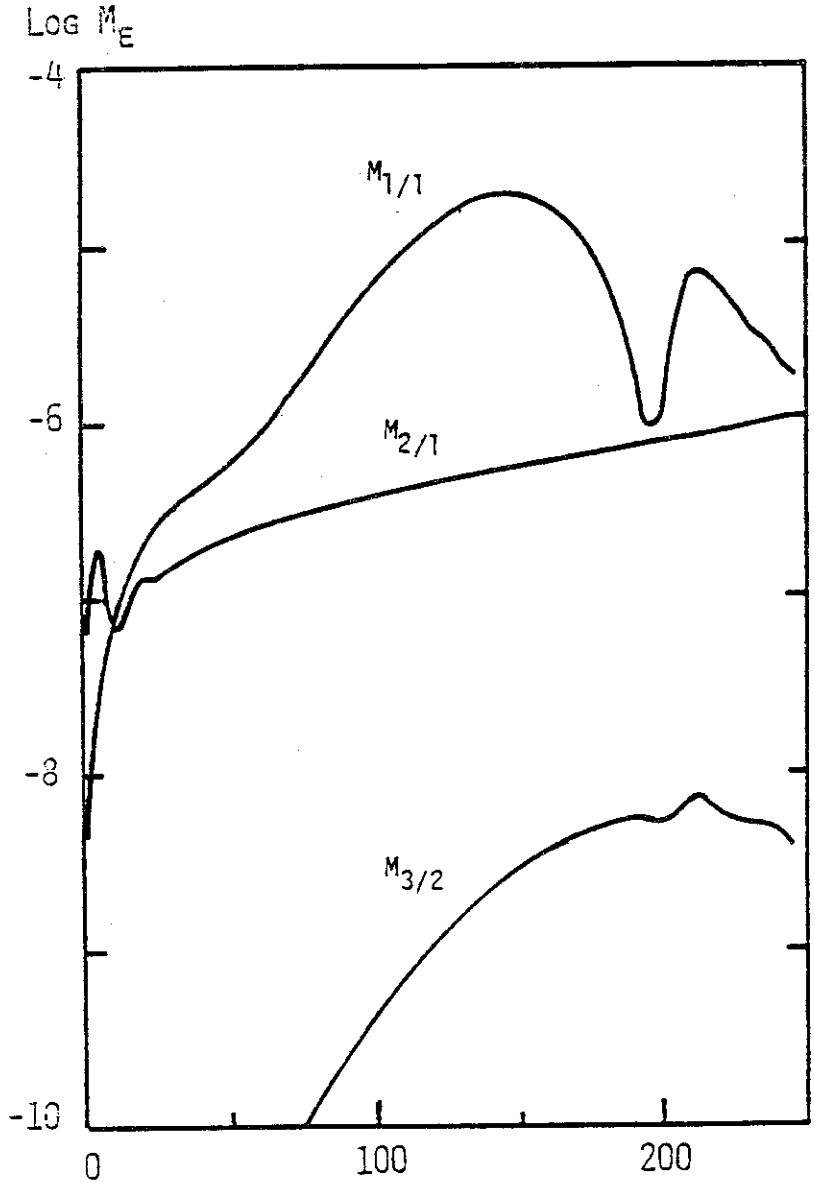

Fig.4.2 (c) Evolution of the m/n mode magnetic energy in a cylindrical plasma.